Hindawi
Mathematical Problems in Engineering
Volume 2022, Article ID 8420722, 9 pages
https://doi.org/10.1155/2022/8420722

Research Article

Emulsion Droplet Pair Coalescence under a Direct Current Electric Field

Muhammad Salman Abbasi,[1] **Husnain Ali**,[1] **Ali Hussain Kazim**,[1] **Tariq Nawaz Chaudhary**,[1,2] **Muhammad Usman**,[1] **Sheraz Afzaal**,[1,3] **Muhammad Usman**,[1] **and Douhadji Abalo**[4]

[1]*Faculty of Mechanical Engineering, University of Engineering and Technology, Lahore 54890, Pakistan*
[2]*School of Engineering and Physical Sciences, Heriot-Watt University, Edinburgh, UK*
[3]*Department of Mechanical Engineering, London South Bank University, London, UK*
[4]*University of Lome, P.O. Box 1515, Lome, Togo*

Correspondence should be addressed to Douhadji Abalo; douhadjiabalo@gmail.com

Received 12 January 2022; Accepted 8 April 2022; Published 2 June 2022

Academic Editor: Muhammad Faisal Nadeem

We investigate the dynamics of the droplet pair coalescence and its stability under a direct current (DC) electric field strength by using simulation and theoretical analyses. We conduct a parametric study to investigate the effects of electric capillary number ($Ca_e = \varepsilon_o \varepsilon_{out} E_o^2 R_o / c$, the ratio of the electrical Maxwell stress to interfacial capillary stress), droplet size ratios (R/R_o, where R and R_o are the radii of the coalescing drops, respectively), and the droplet interfacial separation distance (S) on the coalescence process. We show that unequal-sized droplets undergo unique dynamics owing to the generation of velocity gradient between the coalescing droplets. Moreover, using theoretical analysis, we delineate the stable and unstable regimes of a coalesced droplet under an electric field. Results show that if the semimajor axis of the coalesced droplet becomes greater than 1.5 times, it continuously stretches and becomes unstable. We believe that the study will be useful for essential physical insights pertaining to the coalescence process and valuable for their applications in various areas of biological engineering, chemical sciences, material sciences, and lab on a chip.

1. Introduction

Electrocoalescence of emulsion droplets has wide applications in various fields of engineering and technology including biological engineering [1, 2], chemical sciences [3, 4], electrohydrodynamic printing [5, 6], material sciences [7, 8], and droplet manipulation on lab on a chip [9, 10]. In the petrochemical industry, water in oil emulsions with an average size commonly less than 50 μm is present in crude oil, and electrocoalescence is used for phase separation [11]. An external electric field within a threshold value can be used to trigger or increase the speed of the coalescence. On the other hand, the electric field above a critical value can cause instabilities of droplets rendering the coalescence inefficient or counterproductive [4, 12]. It is therefore very beneficial to develop an essential physical insight and understand the conditions under which the effectiveness of electrocoalescence can be achieved.

Usually, the dispersed and continuous liquids used to study the electrocoalescence process are not perfect dielectrics, and hence, some current leaks through them [13–15]. This leads to a buildup of free charges at the droplet-droplet interface, generation of the tangential stresses, electrohydrodynamic flows, and consequent interface deformation [16–19]. The degree of this deformation is dependent on the dimensionless electric capillary number $Ca_e = (\varepsilon_o \varepsilon_{out} R_o E_0^2 / \gamma)$, where ε_o and ε_{out} are the permittivity of vacuum and relative permittivity of outer liquid, respectively, R_o is droplet radius, γ is interfacial tension, and E_o is unperturbed external electric field while,

simultaneously, the droplets behave like a dipole. Due to the dipolar interaction between them, attractive electrostatic forces $F_e = (-24\pi\varepsilon_o\varepsilon_{\text{out}}R_o^6E_o^2/\overline{S}^4)$ ($\overline{S}$ being the droplet center-to-center separation) are generated which makes them to move closer. During the droplets approach, the medium film between the droplets gets squeezed. When the film thickness reduces to ~100 nm, the film ruptures, and the two droplets coalesce [20–23].

In literature, the earliest study of electrocoalescence was conducted by Berg et al. [24] using two anchored droplets. The subsequent studies were primarily focused on studying the influence of various parameters such as interdroplet separation, droplet radius, type of electric field strength, AC or DC, and/or other physical and electrical properties of the dispersed and continuous liquids [25, 26]. Attens et al. [23] theoretically studied the coalescence of alike droplets placed at a nearby proximity. Brazier-Smith et al. [27] numerically studied two conductive droplets subjected to the influence of electric field strength and investigated that as the separation between the two droplets was in a range $S_o/R_o < 1.2$, where S_0 was the initial droplet center-to-center separation and R was the radius of the droplets, the droplets attract and coalesce. But when $S_o/R_o > 1.2$, it gives rise to a conical shape whose angle was equal to Taylor's cone angle and eventually gives birth to jets of tiny drops. On the other hand, the authors have established the electric capillary number at which a single conducting emulsion droplet becomes unstable to be around 0.20 [28, 29]. Baygents et al. [30] explored the coalescence dynamics and the shapes of equal-sized leaky dielectric droplets (LD) and perfect conducting droplets (PD) with the consideration of droplet deformation and interdroplet separation by using the boundary element method (BEM). Williams and Bailey [31] investigated the coalescence rate of the conducting drops subjected to the influence of electric fields both experimentally and theoretically. Mhatre et al. [32] further considered the electrocoalescence of equal-sized droplet pairs using BEM method with aided experiments. They considered both the LD and PD systems in their analysis. A direct comparison of experiments and numerical results was presented highlighting the droplet-droplet approach and film drainage mechanisms in detail. Recently, electrocoalescence of surfactant-laden droplet pairs in oil and partial coalescence has also been studied [33, 34]. To the best of our information, the existing data are mostly concerned with theoretical analysis (largely numerical), and the droplets of equal size have been mostly considered. Thus, to investigate the droplet approach, coalescence, and stability of the coalesced unequal-sized droplets under an electric field strength, wide-ranging parametric findings are required.

In the current work, we have studied the coalescence of two unequal-/nonuniform-sized droplets. We performed a simulation to find the effect of different parameters including electric capillary number, droplet size ratio, and droplet-droplet interfacial separation distance on the electrocoalescence. We performed theoretical analysis to delineate the stable and unstable regimes of coalescence. To fully understand the behavior of nonuniform-sized droplets under an electric field, the paper is organized as follows: In Section 2, we present the simulation setup. Section 3 concerns with the validation of the simulation model. In Section 4, the detailed results and theoretical analysis are presented. Finally, Section 5 presents the conclusions.

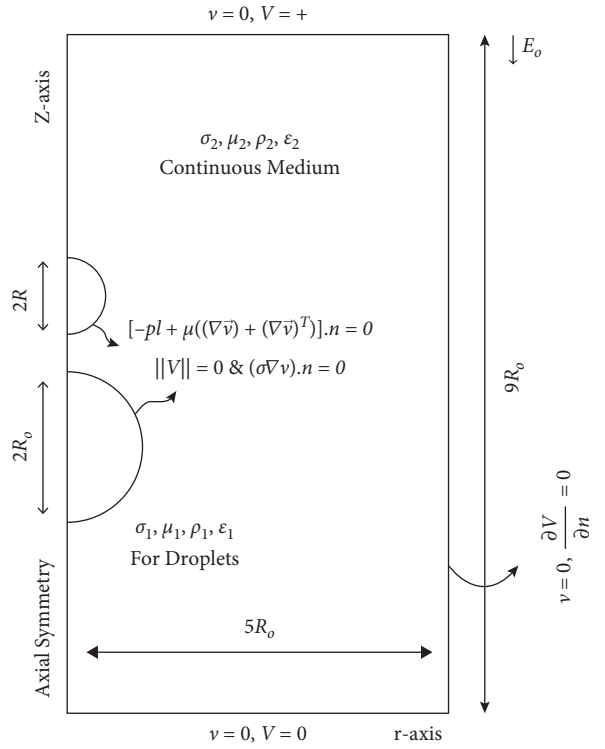

Figure 1: Numerical domain with boundary conditions.

2. Materials and Methods

2.1. Simulation Method. We considered a two-dimensional axisymmetric cylindrical domain to model the problem. The simulation domain with comprehensive boundary settings is given in Figure 1. The height and the radius of this domain were fixed. In this problem, we have considered two droplets of viscosity μ_{in}, electric conductivity σ_{in}, density ρ_{in}, and electric permittivity ε_{in} immersed in a nonmiscible liquid of viscosity μ_{out}, electric conductivity σ_{out}, and density ρ_{out}. The size of one of the droplets was fixed as R_o while the size of the other was varied. The no-slip boundary setting was applied to all the walls of the domain. A DC voltage was applied at the top of the domain while the bottom was grounded. The right wall was electrically insulated.

To observe the combined effects of the hydrodynamic, and the electrical forces during the electrocoalescence process, the problem was solved numerically using the COMSOL Multiphysics 5.3a. Navier-Stokes' equation in conjunction with the fundamental formulations of electroquasi-static physics was solved. The interface of the droplets was traced using the conservative level set method [35]. Here, the applied electric field is $\overrightarrow{E} = -\Delta V$, and the Maxwell stresses are produced at the droplet interfaces expressed as $\varepsilon_0\varepsilon_{\text{out}}(E \cdot \overrightarrow{E} - (E^2I/2))$. The electric force per unit volume is resulted due to the divergence of these

Table 1: Properties of the liquids.

Liquid	Density (kg/m^3)	Viscosity (Pa s)	Dielectric constant	Conductivity ($1/\Omega^{-1}$·m)
Silicone oil	970	0.97	3.2	8.7×10^{-13}
Castor oil	961	0.78	4.7	3×10^{-11}
DI water	998	0.001	78.4	5.5×10^{-5}

Table 2: Simulation systems used to study the electrocoalescence between the droplet pairs.

System	Dispersed phase/continuous phase	Viscosity ratios $\lambda=\mu_{in}/\mu_{out}$	Permittivity ratios $\wp=\varepsilon_{in}/\varepsilon_{out}$	Conductivity ratios $\Re=\sigma_{in}/\sigma_{out}$
1	DI water/silicone oil	10^{-3}	24.5	10^7
2	Castor oil/silicone oil	0.804	1.47	34.48

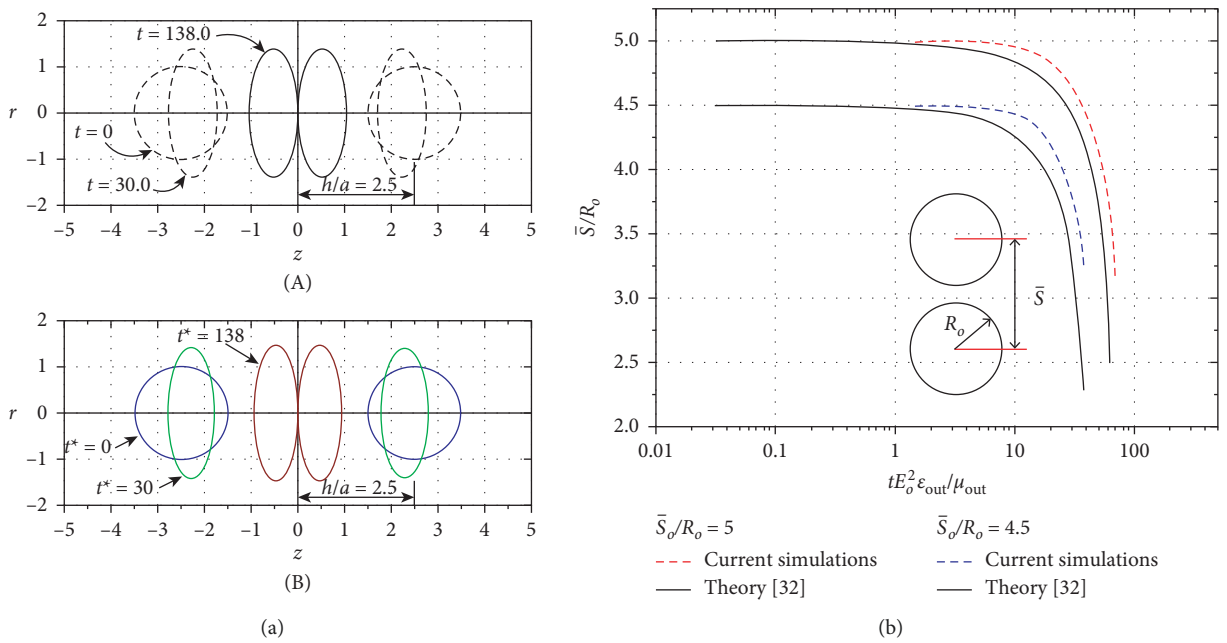

Figure 2: Uniform-sized droplet pair interaction in a uniform DC electric field. (a) (i) Results obtained by Baygents et al. [30]. (ii) Results obtained by our simulation model. The detailed simulation conditions are $\sigma_{in}/\sigma_{out}=2$, $\varepsilon_{in}/\varepsilon_{out}=8$, $\lambda=1$, and $Ca_e=1$. (b) Droplet pair approach at different nondimensionalized time scale obtained from our simulation model and compared with theory [32]. Here, $\bar{S}_o$ is the initial center-to-center distance normalized by the droplet radius R_o, E_o is an unperturbed external electric field strength, and ε_{out} and μ_{out} are the permittivity and viscosity of the outside liquid, respectively.

Maxwell stresses. The detailed core governing equations related to the simulation technique are presented in the supplementary information. The detailed properties of the liquids used in simulations are summarized in Tables 1 and 2.

3. Validation of Simulation Model

To validate our simulation model, we reproduced a few results as reported by Baygents et al. [30] as shown in Figure 2(a) and Figure S1. Baygents et al. used BEM to study the deformation and dynamics of the droplets. The results obtained from our simulation technique were in decent agreement with those reported in the study of Baygents et al. with three different sets of properties of the system. We further validated our simulation modelling against the analytical model [32] for the droplet-droplet approach. The results are shown in Figure 2(b). A reasonable agreement can be seen.

4. Results and Discussion

Herein, we study the droplet pair coalescence under an electric field using simulation and theoretical analysis. Two different systems, aqueous droplet pair in silicone oil and castor droplet pair in silicone oil, are used for the analysis. We changed the various parameters such as electric capillary number (Ca_e), droplet size ratio (R/R_o), and interdroplet distance. We kept the size of one droplet fixed as R_o while the size of another droplet was varied. Moreover, we explored the stability of coalesced droplet.

The driving force in the process of electrocoalescence is the force induced on the droplets which depend upon the Ca_e. Therefore, Ca_e is one of the most important parameters

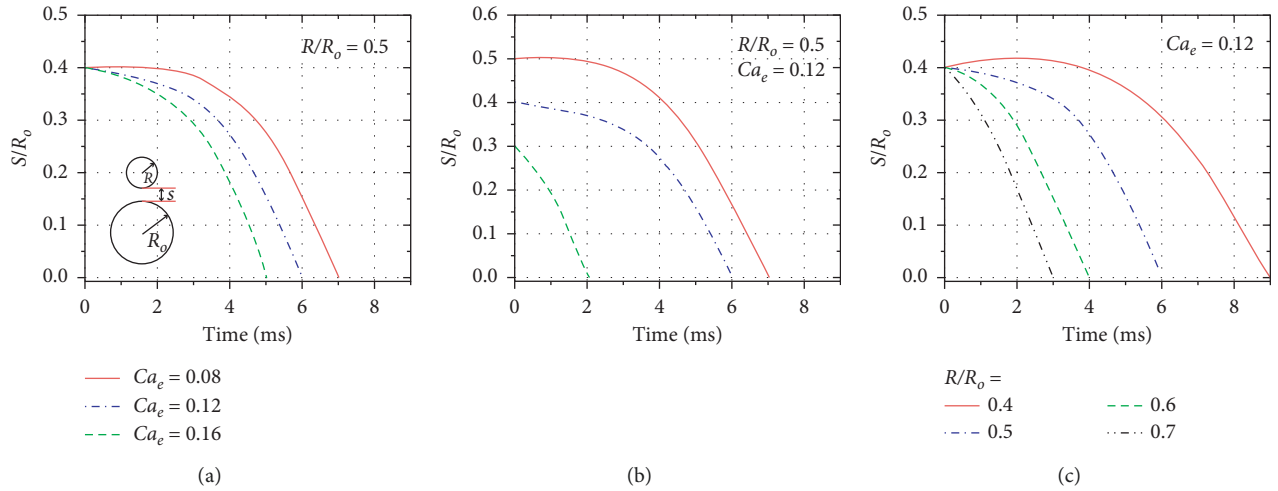

FIGURE 3: Nonuniform sized droplet pair interaction in a uniform DC electric field. (a) Effect of electric capillary number Cae at constant interfacial separation (S). Here, Cae is increased by increasing the electric field strength. (b) Effect of initial separation (S) on the droplet pair approach. (c) Effect of droplet pair radius ratio on the interfacial separation. In (a), (b), and (c), S is the interfacial separation normalized by the radius of the larger droplet, Ro = 1 mm, whereas R is the radius of the smaller droplet. R/Ro is the droplet pair radius ratio. The detailed simulation conditions are $\Re = 107$, $\wp = 24.5$, and $\lambda = 10^{-3}$.

in the electrocoalescence process. The effect of Ca_e was observed by implementing different values of Ca_e in our simulation model. Figure 3(a) shows the nondimensionalized interfacial separation (S/R_o) between the droplets versus time at different values of Ca_e. By increasing the value of Ca_e, the coalescence occurred in lesser time; however, this effect was limited by the critical value of Ca_e that causes the coalescence to become either partial or unstable (will be explained later). Figure 3(b) shows the effect of initial separation on the process of coalescence. These results obtained from the simulation model show that for shorter values of S/R_o, the lesser is the time required to coalesce due to stronger attractive forces between the droplets. Figure 3(c) shows the effect of droplet size ratio (R/R_o) placed at the same initial interfacial separation with constant Ca_e. The results showed that stronger attractive forces were induced for droplets having similar sizes (larger radius ratios) resulting in faster coalescence. However, the effect is reduced in the case of small droplet size ratios as the electric forces become less dominant with a decrease in the size of one of the droplets.

Figures 4(a) and 4(b) show the detailed comparison between the dynamics of the droplet approach and coalescence for equal and unequal-sized droplets. We considered two cases for which $R/R_o = 1$ and $R/R_o = 0.5$ depicting the equal and unequal-sized droplets, respectively. In both cases, the magnitude of the velocity first increases abruptly as the droplets approach each other and then decreases with time as the coalescence is completed. As the equal-sized droplets coalesce, a uniform velocity field inside the two droplets was observed (see Figure 4(a)). However, the smaller droplet displayed a larger velocity in the case of unequal-sized droplets (see Figure 4(b)). Thus, a velocity differential was observed that altered the coalescence dynamics. As a consequence of this, the smaller droplet merged more abruptly into the larger droplet. We performed extensive simulations to predict the magnitude of this velocity differential over a range of different droplet size ratios. Figure 4(c) shows the velocity differential versus time for the cases having different values for R/R_o at the same values for Ca_e and initial separation. Here, the time is measured from the instant of the onset of the interface collapse. As the interfaces start to merge, a large velocity differential occurs between the centers of the two merging droplets that decrease with a rapid expansion in the liquid bridge. Ultimately, the velocity differential diminishes at the termination of coalescence. With an increase in the droplet size ratio, the velocity differential keeps on decreasing and ultimately vanishes for equal-sized droplets.

The pressure contours are as shown in Figures 5(a) and 5(b). A pressure differential exists in the case of the unequal-sized droplet. This pressure differential decreases with a decrease in droplet size ratios as shown in Figure 5(c). As the Laplace pressure ($\Delta P = 2\gamma/R$) is inversely proportional to the radius of the droplet, the smaller droplet will have greater pressure inside it.

For the given scenario in Figure 5(b), the Laplace pressure differential between the two droplets is ~36 Pa ($R = 0.5$ mm and $R_o = 1$ mm, $\gamma = 0.018$ N/m). Simulations also show a pressure gradient of ~40 Pa for this case at the onset of interface collapse. However, after the interfaces collapse with one another, an abrupt increase in pressure differential is observed. This was due to the combined effect of the Laplace pressure differential and the electrostatic forces accelerating the coalescence process. This implies that a smaller droplet with a greater Laplace pressure should merge into a larger droplet faster compared to equal-sized droplets resulting in a production of a pressure jet.

We next explored the phenomenon of stable and unstable coalescence. Figure 6(a) shows droplet coalescence led to stable coalesced droplets or the coalesced droplet became unstable, continuously stretched after the merger, and began to eject droplets at the side ends. In order to understand the

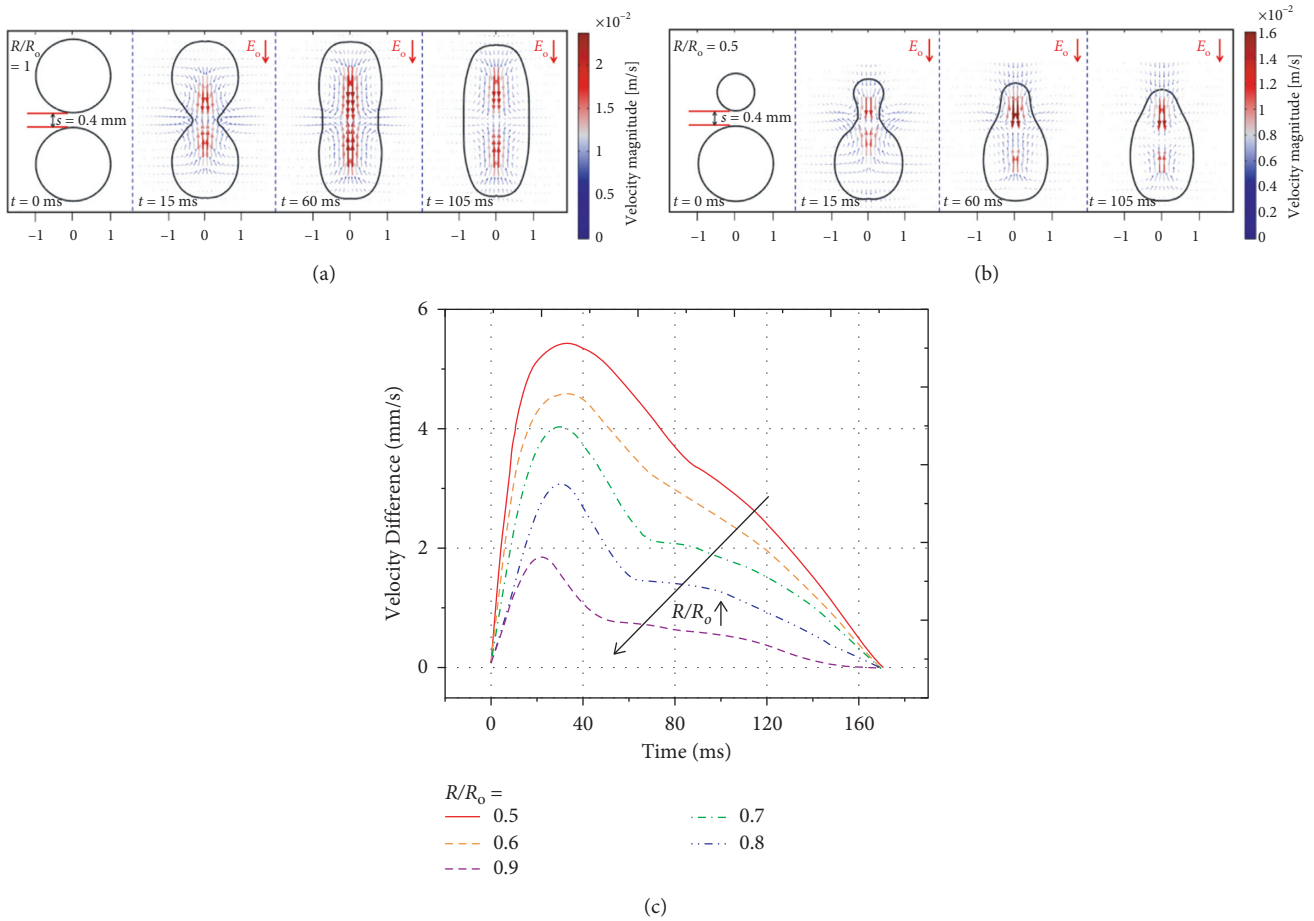

FIGURE 4: Dynamics of the droplet pair approach leading to the process of coalescence in a uniform DC electric field. (a) Velocity vector field at different time intervals for the uniform-sized droplet pair, R/Ro = 1. (b) Velocity vector field at different time intervals for the nonuniform-sized droplet pair, R/Ro = 0.5. Color legend shows the magnitude of velocity. (c) Effect of the droplet pair radius ratio, R/Ro, on the velocity difference between the centers of the nonuniform-sized droplet pair during the coalescing process. Here, the time is measured from the instant of the onset of the droplet pair interface coalescence/merger. For (a), (b), and (c), Cae = 0.12 and initial interfacial separation = 0.4 mm. The detailed simulation conditions are $\Re = 107$, $\wp = 24.5$, and $\lambda = 10^{-3}$.

occurrence of stable and unstable coalescence and to delineate the two regimes within the perspective of droplet size ratios under an electric field, we have undergone a theoretical analysis. We considered a merged or coalesced droplet and calculated the electrical Maxwell stresses (P_E) and the change in capillary stresses (P_c) at the side apex point C ($\theta = 0$) as shown in Figure 6(b). The coalesced droplet stretched due to the interfacial electric stresses acting at the interface under an electric field; thus,

$$P_c \simeq P_E. \tag{1}$$

The change in the electric capillary stresses of the merged droplet stretching is given as [36]

$$P_c = P_f - P_i = \gamma\left(\frac{8}{\alpha} - \frac{6r}{\alpha^2}\right) - \left(\frac{2\gamma}{r}\right), \tag{2}$$

where α and r are the length of the semimajor axis of the deformed and undeformed configurations of a coalesced droplet. Electric stresses acting at the side apex point ($\theta = 0$) can be given as [15]

$$P_E \sim \kappa \frac{\varepsilon_o \varepsilon_{\text{out}} E_o^2}{((2/\Re)+1)^2}\left[\left(1 - \frac{\wp}{\Re^2}\right)\right] = \kappa \frac{\varepsilon_o \varepsilon_{\text{out}} E_o^2}{((2/\Re)+1)^2}\left[\left(1 - \frac{\wp}{\Re^2}\right)\right],$$
$$P_E \sim \kappa \frac{\varepsilon_o \varepsilon_{\text{out}} E_o^2}{(2+\Re)^2}\left[\left(\Re^2 - \wp\right)\right], \tag{3}$$

where $\Re$ and $\wp$ are the conductivity ratio and permittivity ratio between the droplet and the outside liquid, respectively.

Substituting the expressions of change in capillary stresses and electric stresses in (1) gives

$$2\gamma\left(\frac{4}{\alpha} - \frac{-3r}{\alpha^2}\right) - \left(\frac{2\gamma}{r \simeq \kappa}\right)\frac{\varepsilon_o \varepsilon_{\text{out}} E_o^2}{(2+\Re)^2}\left[\left(\Re^2 - \wp\right)\right]. \tag{4}$$

Multiplying both sides of (4) by r/γ yields

$$2\left(\frac{4}{\alpha^*} - \frac{3}{\alpha^{*2}}\right) \simeq \kappa \frac{\varepsilon_o \varepsilon_{\text{out}} E_o^2 r}{(2+\Re)^2 \gamma}\left[\left(\Re^2 - \wp\right)\right] + 2. \tag{5}$$

Here, $r = (R_o^3 + R^3)^{1/3} = R_o(1 + (R^3/R_o^3))^{1/3}$.

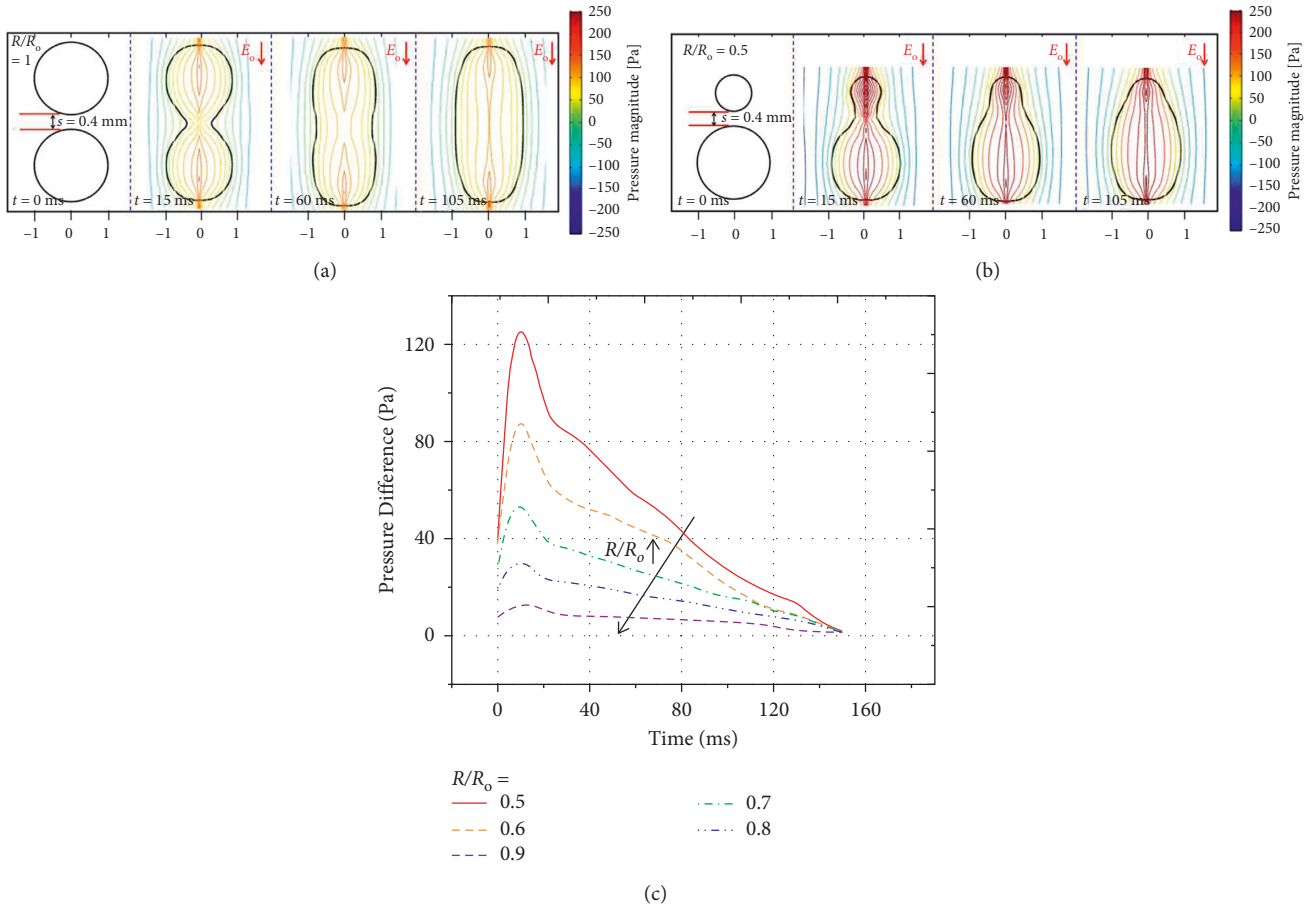

Figure 5: Pressure characteristics of the droplet pair approach leading to the process of coalescence in a DC uniform electric field. (a) Pressure contours at different time intervals for uniform sized droplet pair, $R/R_o = 1$. (b) Pressure contours at different time intervals for nonuniform sized droplet pair, R/Ro = 0.5. Color legend shows the magnitude of the pressure. (c) Effect of the radius ratio, R/Ro, on the pressure difference between the centers of the nonuniform-sized droplet pair during the coalescing process. Here, the time is measured from the instant of the onset of the droplet pair interface coalescence/merger. For (a), (b), and (c), $Ca_e = 0.12$, and initial interfacial separation = 0.4 mm. The detailed simulation conditions are $\Re = 107$, $\wp = 24.5$, and $\lambda = 10^{-3}$.

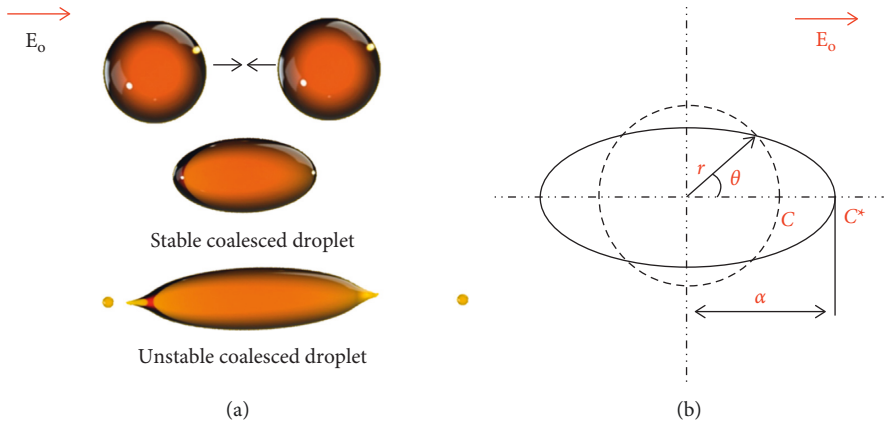

Figure 6: (a) Coalescence led to stable or unstable droplet configurations under an electric field. (b) Schematic of the coalesced droplet stretching and the movement of the point C ($\theta = 0$) at the side end to a new position, C ∗ . r represents the radius of the undeformed droplet, and α represents the length of the semimajor axis of the deformed droplet.

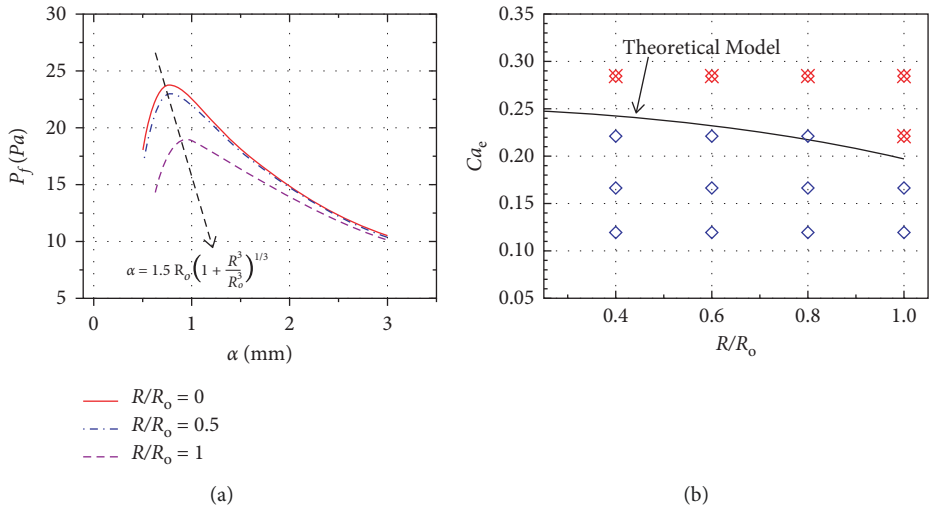

FIGURE 7: (a) Change in the capillary pressure with a coalesced droplet stretching at different droplet pair radius ratios. Coalesced droplet becomes unstable if $\alpha \gtrsim 1.5R_o\,(1 + (R^3/R_o^3))^{1/3}$. (b) Critical electric capillary number for the onset of instability of the coalesced droplet at different droplet pair radius ratios. Blue open diamond symbols show stable complete coalescence whereas red crossed diamond symbols show unstable coalescence. Here, a solid line is obtained from equation (9) depicting the onset of unstable coalescence. Open and crossed symbols are simulation results for the castor oil droplet pair coalescence in the silicone oil. A reasonably good agreement is observed between theory and simulations.

$$2\left(\frac{4}{\alpha^*}-\frac{3}{\alpha^{*2}}\right)\simeq\kappa Ca_e^*\frac{\left[\left(\Re^2-\wp\right)\right]}{(2+\Re)^2}+2, \tag{6}$$

where

$$Ca_e^*=\frac{\varepsilon_o\varepsilon_{\text{out}}E_o^2R_o\left(1+R^3/R_o^3\right)^{1/3}}{\gamma},$$
$$\alpha^*=\left(\frac{\alpha}{R_o}\right)\left(1+\frac{R^3}{R_o^3}\right)^{1/3}, \tag{7}$$

and

$$Ca_e^*=Ca_{e,\text{crit}}\left(1+\frac{R^3}{R_o^3}\right)^{1/3}, \tag{8}$$

$$2\left(\frac{4}{\alpha^*}-\frac{3}{\alpha^{*2}}\right)\simeq\kappa Ca_{e,\text{crit}}\left(1+\frac{R^3}{R_o^3}\right)^{1/3}\frac{\left[\left(\Re^2-\wp\right)\right]}{(2+\Re)^2}+2. \tag{9}$$

The critical condition for the delineation between stable and unstable coalesced droplet regimes was revealed by the plot of the capillary-stress term (P_f) from (2). This term initially increases with an increase in coalesced droplet major axis (α) to resist the deformation induced by the electrical stresses. Though, it inclines to a decline if $\alpha \gtrsim 1.5R_o\,(1 + (R^3/R_o^3))^{1/3}$, as presented in Figure 7(a). We solved (9) using the substitution method by incorporating the condition of instability to find the critical values of Ca_e under different conditions of droplet size ratios (R/R_o) for the onset of unstable coalescence as shown in Figure 7(b). Thus, if the semimajor axis of the coalesced droplet is less than 1.5 times that of its undeformed configuration, then it will remain stable. However, if the semimajor axis tends to become larger than 1.5 times, it continuously stretches and becomes unstable.

We further performed extensive simulations to verify the theoretical results at different droplet size ratios of the castor droplet in silicone oil. A good agreement can be seen between the theory and the simulation for a value of $\kappa = 3$. Figure 7(b) provides a delineation between the two regimes in a droplet's radius ratio (R/R_o) versus electric capillary number (Ca_e) parametric space.

5. Conclusions

Here, we extensively studied the effect of various parameters such as electric capillary number, droplet size ratio, and interfacial separation on the droplet-droplet approach and consequent coalescence. The simulation model was validated against the analytical and numerical results of other researchers. Based on extensive numerical analysis, we established a unique dynamic of coalescence of unequal-sized droplets within the perspective of velocity and pressure characteristics. Moreover, a rigorous theoretical analysis was performed to understand the stability of a coalesced droplet at varying conditions of electric capillary number and droplet size ratios. After exploring the critical conditions of instability, we presented a diagram delineating the stable and unstable regimes of the coalesced droplet. The results show that the unequal-sized droplets undergo unique dynamics owing to the generation of velocity gradient between the coalescing droplets. The theoretical model establishes that as the coalesced droplet major axis (α) becomes $\gtrsim 1.5R_o\,(1+ (R^3/R_o^3))^{1/3}$, the instability onsets and daughter droplets are ejected from the side apex. Furthermore, a future study to explore the daughter droplet's shape and its characteristics could be an interesting one.

We believe that this study has the potential to offer an opportunity to comprehend the coalescence dynamics of unequal-sized droplets under an electric field. This will offer outstanding prospects for the comprehension of their functionalities in various areas of science and technology.

Data Availability

The data used to support the findings of this study are included in this paper.

Disclosure

Muhammad Salman Abbasi and Husnain Ali are cofirst authors.

Conflicts of Interest

The authors declare that they have no conflicts of interest.

Authors' Contributions

Muhammad Salman Abbasi and Husnain Ali contributed equally.

Acknowledgments

Muhammad Salman Abbasi and Ali Turab Jafry would like to thank Higher Education Commission (HEC), Pakistan, for funds under Technology Transfer Support Fund (HEC-TTSF-74).

Supplementary Materials

The supplementary file contains details about the governing equations implemented in the numerical simulation and numerical model validation results. (*Supplementary Materials*)

References

[1] N. Hu, J. Yang, S. W. Joo, A. N. Banerjee, and S. Qian, "Cell electrofusion in microfluidic devices a review," *Sensors and Actuators B: Chemical*, vol. 178, pp. 63–85, 2013.

[2] R. Dimova, N. Bezlyepkina, M. D. Jordö et al., "Vesicles in electric fields: some novel aspects of membrane behavior," *Soft Matter*, vol. 5, no. 17, pp. 3201–3212, 2009.

[3] T. Leary, M. Yeganeh, and C. Maldarelli, "Microfluidic study of the electrocoalescence of aqueous droplets in crude oil," *ACS Omega*, vol. 5, no. 13, pp. 7348–7360, 2020.

[4] S. Mhatre, V. Vivacqua, M. Ghadiri et al., "Electrostatic phase separation: a review," *Chemical Engineering Research and Design*, vol. 96, pp. 177–195, 2015.

[5] T. Seifert, E. Sowade, F. Roscher, M. Wiemer, T. Gessner, and R. R. Baumann, "Additive manufacturing technologies compared: morphology of deposits of silver ink using inkjet and aerosol jet printing," *Industrial & Engineering Chemistry Research*, vol. 54, no. 2, pp. 769–779, 2015.

[6] V. D. Nguyen and D. Byun, "Mechanism of electrohydrodynamic printing based on ac voltage without a nozzle electrode," *Applied Physics Letters*, vol. 94, no. 17, Article ID 173509, 2009.

[7] Z. Rozynek, A. Mikkelsen, P. Dommersnes, and J. O. Fossum, "Electroformation of Janus and patchy capsules," *Nature Communications*, vol. 5, no. 1, p. 3945, 2014.

[8] X. T. Sun, C. G. Yang, and Z. R. Xu, "Controlled production of size-tunable Janus droplets for submicron particle synthesis using an electrospray microfluidic chip," *RSC Advances*, vol. 6, no. 15, Article ID 12047, 2016.

[9] Y. Jia, Y. Ren, W. Liu et al., "Electrocoalescence of paired droplets encapsulated in double-emulsion drops," *Lab on a Chip*, vol. 16, no. 22, pp. 4313–4318, 2016.

[10] R. Song, M. S. Abbasi, and J. Lee, "Fabrication of 3D printed modular microfluidic system for generating and manipulating complex emulsion droplets," *Microfluidics and Nanofluidics*, vol. 23, no. 7, 92 pages, 2019.

[11] S. Less and R. Vilagines, "The electrocoalescers' technology: advances, strengths and limitations for crude oil separation," *Journal of Petroleum Science and Engineering*, vol. 81, pp. 57–63, 2012.

[12] D. Yang, M. Ghadiri, Y. Sun, L. He, X. Luo, and Y. Lü, "Critical electric field strength for partial coalescence of droplets on oil-water interface under DC electric field," *Chemical Engineering Research and Design*, vol. 136, pp. 83–93, 2018.

[13] G. I. Taylor, "Disintegration of water drops in an electric field," *Proceedings of the Royal Society of London - Series A: Mathematical and Physical Sciences*, vol. 280, no. 1382, pp. 383–397, 1964.

[14] G. I. Taylor, "Studies in electrohydrodynamics I The circulation produced in a drop by electrical field," *Proceedings of the Royal Society of London - Series A: Mathematical and Physical Sciences*, vol. 291, no. 1425, pp. 159–166, 1966.

[15] S. Torza, R. G. Cox, and S. G. Mason, "Electrohydrodynamic deformation and bursts of liquid drops," *Philosophical Transactions of the Royal Society of London - A*, vol. 269, no. 1198, pp. 295–319, 1971.

[16] M. S. Abbasi, R. Song, H. Kim, and J. Lee, "Multimodal breakup of a double emulsion droplet under an electric field," *Soft Matter*, vol. 15, no. 10, pp. 2292–2300, 2019.

[17] O. Ajayi, "A note on Taylor's electrohydrodynamic theory," *Proceedings of the Royal Society of London A*, vol. 364, no. 1719, pp. 499–507, 1978.

[18] N. Bentenitis and S. Krause, "Droplet deformation in dc electric fields: the extended leaky dielectric model," *Langmuir*, vol. 21, no. 14, pp. 6194–6209, 2005.

[19] E. K. Zholkovskij, J. H. Masliyah, and J. Czarnecki, "An electrokinetic model of drop deformation in an electric field," *Journal of Fluid Mechanics*, vol. 472, pp. 1–27, 2002.

[20] J. Latham and I. W. Roxburgh, "Disintegration of pairs of water drops in an electric field," *IEEE Transactions on Industry Applications*, vol. 295, no. 1440, pp. 84–97, 1966.

[21] J. Raisin, P. Atten, F. Aitken, and J. L. Reboud, "Electrically induced coalescence of two facing anchored water drops in oil," in *Proceedings of the 2008 IEEE International Conference on Dielectric Liquids*, Chasseneuil, France, July 2008.

[22] P. Atten, "Critical conditions for electrically induced coalescence of two very close water droplets in oil," in *Proceedings of the IEEE International Conference on Dielectric Liquids*ICDL 2005. 2005, Coimbra, Portugal, July 2005.

[23] P. Atten, L. Lundgaard, and G. Berg, "A simplified model of electrocoalescence of two close water droplets in oil," *Journal of Electrostatics*, vol. 64, no. 7-9, pp. 550–554, 2006.

[24] T. G. Owe Berg, G. C. Fernish, and T. A. Gaukler, "The mechanism of coalescence of liquid drops," *Journal of the Atmospheric Sciences*, vol. 20, no. 2, pp. 153–158, 1963.

[25] P. Atten, "Electrocoalescence of water droplets in an insulating liquid," *Journal of Electrostatics*, vol. 30, pp. 259–269, 1993.

[26] G. M. Panchenkov and V. M. Vinogradov, "Water-in-oil emulsion in a constant homogeneous electric field," *Chemistry and Technology of Fuels and Oils*, vol. 6, no. 6, pp. 438–441, 1970.

[27] P. R. Brazier-Smith, S. G. Jennings, and J. Latham, "An investigation of the behaviour of drops and drop-pairs subjected to strong electrical forces," *Proceedings of the Royal Society of London. A. Mathematical and Physical Sciences*, vol. 325, no. 1562, pp. 363–376, 1971.

[28] E. Lac and G. M. Homsy, "Axisymmetric deformation and stability of a viscous drop in a steady electric field," *Journal of Fluid Mechanics*, vol. 590, pp. 239–264, 2007.

[29] H. Paknemat, A. R. Pishevar, and P. Pournaderi, "Numerical simulation of drop deformations and breakup modes caused by direct current electric fields," *Physics of Fluids*, vol. 24, no. 10, Article ID 102101, 2012.

[30] J. C. Baygents, N. J. Rivette, and H. A. Stone, "Electrohydrodynamic deformation and interaction of drop pairs," *Journal of Fluid Mechanics*, vol. 368, pp. 359–375, 1998.

[31] T. J. Williams and A. G. Bailey, "Changes in the size distribution of a water-in-oil emulsion due to electric field induced coalescence," *IEEE Transactions on Industry Applications*, vol. IA-22, no. 3, pp. 536–541, 1986.

[32] S. Mhatre, S. Deshmukh, and R. M. Thaokar, "Electrocoalescence of a drop pair," *Physics of Fluids*, vol. 27, no. 9, Article ID 092106, 2015.

[33] X. Luo, H. Yin, H. Yan, X. Huang, D. Yang, and L. He, "The electrocoalescence behavior of surfactant-laden droplet pairs in oil under a DC electric field," *Chemical Engineering Science*, vol. 191, pp. 350–357, 2018.

[34] V. Vivacqua, M. Ghadiri, A. M. Abdullah et al., "Analysis of partial electrocoalescence by Level-Set and finite element methods," *Qatar Foundation Annual Research Conference*, vol. 114, pp. 180–189, 2016.

[35] E. Olsson, G. Kreiss, and S. Zahedi, "A conservative level set method for two phase flow II," *Journal of Computational Physics*, vol. 225, no. 1, pp. 785–807, 2007.

[36] M. S. Abbasi, R. Song, and J. Lee, "Breakups of an encapsulated surfactant-laden aqueous droplet under a DC electric field," *Soft Matter*, vol. 15, no. 43, pp. 8905–8911, 2019.